

RESEARCH ARTICLE

Open Access



Genome sequence of the potato pathogenic fungus *Alternaria solani* HWC-168 reveals clues for its conidiation and virulence

Dai Zhang¹, Jia-Yu He¹, Parham Haddadi², Jie-Hua Zhu^{1*}, Zhi-Hui Yang^{1*} and Lisong Ma^{1*}

Abstract

Background: *Alternaria solani* is a known air-born deuteromycete fungus with a polycyclic life cycle and is the causal agent of early blight that causes significant yield losses of potato worldwide. However, the molecular mechanisms underlying the conidiation and pathogenicity remain largely unknown.

Results: We produced a high-quality genome assembly of *A. solani* HWC-168 that was isolated from a major potato-producing region of Northern China, which facilitated a comprehensive gene annotation, the accurate prediction of genes encoding secreted proteins and identification of conidiation-related genes. The assembled genome of *A. solani* HWC-168 has a genome size 32.8 Mb and encodes 10,358 predicted genes that are highly similar with related *Alternaria* species including *Alternaria arborescens* and *Alternaria brassicicola*. We identified conidiation-related genes in the genome of *A. solani* HWC-168 by searching for sporulation-related homologues identified from *Aspergillus nidulans*. A total of 975 secreted protein-encoding genes, which might act as virulence factors, were identified in the genome of *A. solani* HWC-168. The predicted secretome of *A. solani* HWC-168 possesses 261 carbohydrate-active enzymes (CAZY), 119 proteins containing RxLx[EDQ] motif and 27 secreted proteins unique to *A. solani*.

Conclusions: Our findings will facilitate the identification of conidiation- and virulence-related genes in the genome of *A. solani*. This will permit new insights into understanding the molecular mechanisms underlying the *A. solani*-potato pathosystem and will add value to the global fungal genome database.

Keywords: *Alternaria solani*, Genome sequence, Secretome, Conidiation, Virulence

Background

Alternaria, a genus of ascomycete fungi, causes various disease symptoms, including root and stem rot, blight, and wilt on most economically important plants [1]. *Alternaria solani* is known as the causal agent of early blight of potato and tomato. Early blight of potato is a major foliar disease that is considered one of the most destructive diseases of potato worldwide, resulting in severe yield losses in many potato growing regions [1].

Understanding the factors influencing spore formation and identification of a wide range of secondary metabolites produced by *A. solani* have been the subject of extensive studies in the past many years. For example, Brian et al. first reported that Alternaric acid is a biologically active product of the fungus *Alternaria solani* [2, 3]. In addition, *A. solani* is capable of producing extracellular polysaccharides, carbohydrases, proteases, the new zinniol-related phytotoxins [4, 5], and other secondary metabolites during infection [6, 7]. It has been documented that sporulation of *A. solani* depends upon many factors such as mycelial wounding, temperature, visible light, water treatment, ozone and ultraviolet [8–11]. Growth characteristics, genetic and pathogenic variations of *A. solani* have

* Correspondence: zhujiéhua356@126.com; bdyjh@hebau.edu.cn; lisong.ma@anu.edu.au

¹Center of Plant Disease and Plant Pests of Hebei Province, College of Plant Protection, Hebei Agricultural University, Baoding 071001, China
Full list of author information is available at the end of the article



been studied as well [12–17]. Based on these successful and progressive studies on *A. solani*, the interaction between *A. solani* and its host represents an excellent system that will enable researchers to study the pathogenic mechanisms between *Alternaria* species and their hosts.

Conidiation (asexual sporulation) in filamentous ascomycetous fungi is a complex process involving the formation of conidia on conidiophores [18]. Many studies have been conducted to investigate the sporulation process, resulting in the identification of various environmental factors influencing sporulation, such as light, salt and nutrients and endogenous biological rhythms, but the light is regarded as one of the key environmental factors for regulating sporulation [19]. The molecular basis underlying the conidiation of *Aspergillus nidulans* and *Neurospora crassa* has been well studied, leading to the identification of a set of genetic regulators controlling the asexual sporulation in *A. nidulans* [20–22]. Activation of the transcription factor *brlA* gene by light has been demonstrated as an essential step of conidiation in *A. nidulans* [22, 23]. *abaA* gene is activated by BrlA and loss of *abaA* results in the formation of supernumerary tiers of cells with abacus-like structures [18, 24]. *wetA* gene induced by AbaA during the late stage of conidiation activates a set of genes responsible for the synthesis of cell wall layers and spore specific functions [25, 26]. These three sequentially expressed genes including *brlA*, *abaA* and *wetA* comprise a central regulatory pathway that controls the sporulation in *A. nidulans* [18, 24]. In addition to these three genes, six upstream developmental activators (*fluG*, *flbA*, *flbB*, *flbC*, *flbD* and *flbE*) have been identified by genetic studies on recessive mutations to cause defective conidiation [27]. StuA regulates transcription of the *brlA* gene and plays a key role in the structure and cell morphogenesis during the sexual and asexual phases of reproduction in *A. nidulans* [28, 29]. Previous studies have reported that nutrition, light spectrum and temperature are major factors that influence the sporulation of *A. solani* in vitro; however, the production of conidiospores is limited and variable among distinct isolates of *A. solani* and there is no a common practical protocol developed for the species. Therefore, understanding the molecular mechanism underlying the conidiation of *A. solani* is urgently required.

Advances in next-generation sequencing (NGS) technologies are transforming biology research. The large-scale studies of fungal genome sequence have facilitated the discovery of molecular mechanisms underlying the virulence in plant fungal pathogens. Recently, several genome sequences of *A. solani* isolates have been reported including BMP0185, CBS109157 and altNL03003 [30–32]. Interestingly, the genome of *A. solani* altNL03003 isolated from a Dutch potato field has been sequenced using the long-read Pacific Biosciences (PacBio) sequencing technology. This has provided a gapless genome assembly and produced a

genome size of 32.8 Mb [32]. The available *Alternaria* genome sequence database provides a useful resource to browse and visualize whole genome alignments, genome annotations, and identify homologous genes within the important saprophytic and plant/human pathogenic fungal genus [18, 33–36]. However, a detailed genome annotation and prediction of genes encoding secreted proteins remain unknown for *A. solani*, especially in the genome of *A. solani* isolate from China. Here, we present an accurate genome annotation and provide a prediction of conidiation and effector candidate genes from *A. solani* HWC-168, which holds the potential to advance our understanding of pathogenic mechanisms of *A. solani*.

Results

Genome sequencing and assembly

To gain a better understanding of *A. solani* genome, we generated a high-quality genome sequence of *A. solani* HWC-168 using an Illumina HiSeq 2000 sequencing platform. The high quality of genomic DNA isolated from the mycelium of *A. solani* HWC-168 was used to prepare libraries. Two independent DNA libraries were constructed: one with insert size 500 bp and second one with 5 kb insert size. Total 21.9 Gb and 33.7 Gb of high quality reads were generated from 500 bp library and 5 kb library, respectively. The genome coverage was 200-fold in the library containing insert size 500 bp and 308-fold in the library with 5 kb insert size. The reads generated from both libraries were assembled into 209 contigs and 61 scaffolds, among which the size of the longest scaffold was 5,423,972 bp and scaffold N50 having the size of 2,613,338 bp. The assembled genome size achieved was 32,838,780 bp, which agrees favorably with the reported genome size of *A. solani* of 32.6 to 32.9 Mb [31, 32]. The GC content of the genome was 51.20% of the total bases (Table 1).

Repeat content in *A. solani* HC-168

To characterize the assembled genome, the repetitive elements were identified using the CENSOR prediction. In total, 24,896 repeat elements including DNA transposon, endogenous retrovirus, LTR retrotransposon, non-LTR retrotransposon, pseudogene, satellite and integrated virus were identified in the genome (Table 2). Our analysis revealed that the repeat content accounted for 6.95% of the genome in length, which differs with that of *A. solani* CBS109157 [31]. The distribution of LTR retrotransposon was heavily dominant (3.3% of the entire genome) but DNA transposon (2.43%), Non-LTR retrotransposon (0.91%) and endogenous retrovirus (0.21%) were also highly represented. Based on the superfamily types, most common types of repetitive elements were represented in the *A. solani* genome with the dominant family being Gypsy (2.7% of the genome) and the most

Table 1 Summary of genome assembly and annotation features of *A. solani*, *A. arborescens* and *A. brassicicola*

	<i>A. arborescens</i> EGS39–128	<i>A. brassicicola</i> ATCC 96836	<i>A. solani</i> HWC-168	<i>A. Solani</i> altNL03003
Genome				
Isolate	EGS 39–128	ATCC 96836	HWC-168	altNL03003
Coverage (fold)	90	6.4	508	> 150
Genome size	33,889,384 bp	29,536,471 bp	32,838,780 bp	32,779,142 bp
No. of contigs	1332	4039	209	10
Largest contig length	1,056,452 bp	87,976 bp	1,075,562 bp	7,235,174 bp
N50 contig length	310,869	18,835	564,368	
G + C content (%)	50.9	50.7	51.2	51.2
Genes				
Number of genes	11,042	10,514	10,358	
Gene density(genes/Mb)	325	356	323	
Number of specific genes	1689	1883	1632	

abundant family being Copia (0.67%) and EnSpm/CACT A (0.60%) and Mariner/Tc1 (0.45%).

Comparison of genome assembly features within *Alternaria* species

The genome size of *A. solani* HWC-168 (32.8 Mb) was small compared to *A. arborescens* (33.9 Mb) but larger than *A. brassicicola* (29.5 Mb) [30]. It has approximately the same size as reported for *A. solani* altNL03003 (32.8 Mb) [32]. The average gene density in *A. solani* HWC-168 genome was 323 genes per Mb, which remains lower than that in *A. brassicicola* (356 genes per Mb) and *A. arborescens* (325 genes per Mb). Next, we compared the whole genome assembly features of *A. solani* HWC-168 with those of sequenced *A. arborescens* EGS 39–128, *A. brassicicola* ATCC 96836 and *A. solani* altNL03003 genomes (Table 1). Compared to *A. arborescens* and *A. brassicicola*, our genome assembly was superior because it featured the greatest genome coverage, the minimum number of contigs and largest N50 contig length (Table 1). However, compared to *A. solani* altNL03003, a large number of contigs was observed in our assembly (Table 1). In addition, we compared the gene distribution in the three annotated *A. brassicicola*, *A. arborescens* and *A. solani* HWC-168 genomes by calculating the intergenic distance between adjacent genes. Figure 1 showed that the distributions of intergenic distances in *A. solani* HWC-168 genome were similar to those in the genome of *A. brassicicola*. However, the distributions of intergenic distances in *A. arborescens* genome were less variable and genes in *A. arborescens* genome were more closely spaced than the analyzed *A. solani* and *A. brassicicola* genomes (Fig. 1).

Gene prediction and functional annotation

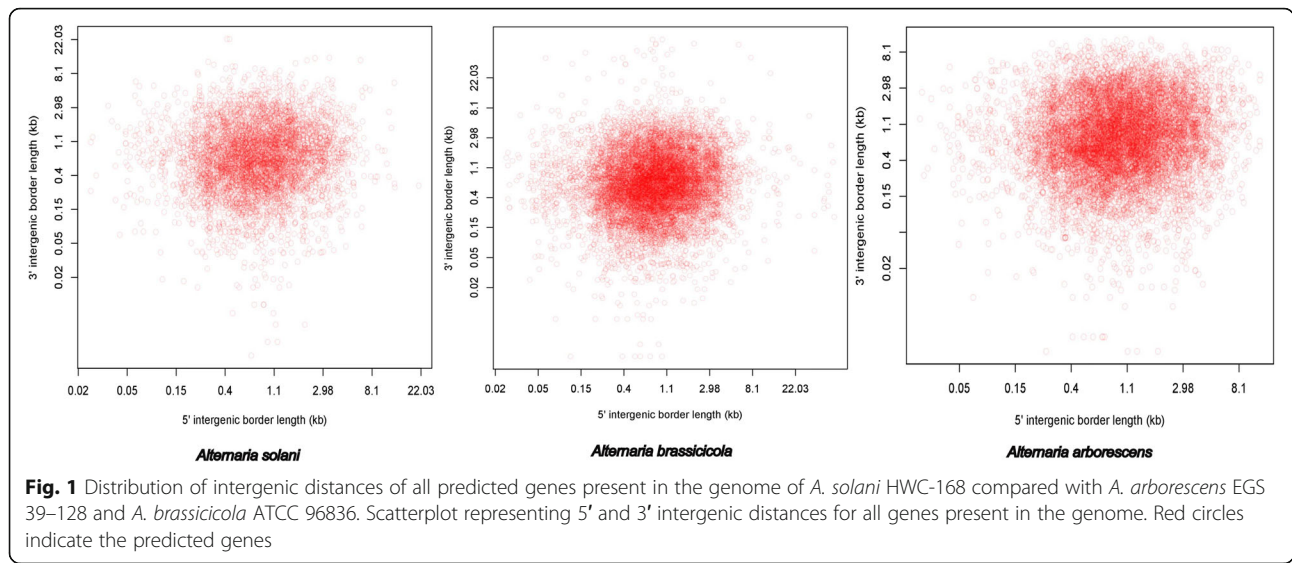
To predict complete genes in *A. solani* HWC-168 genome, we used the Augustus version 2.5.5 [53]. The

analysis resulted in 10,358 complete genes in the genome of *A. solani* HWC-168. PanOCT analysis was employed to examine the orthologous gene clusters among predicted genes of *A. solani* HWC-168, *A. arborescens* EGS 39–128 and *A. brassicicola* ATCC 96836. The total number of predicted genes, core genes, clusters of orthologous groups (COGs) and shared COGs were summarized in the Venn diagram for ortholog clusters in these three genomes (Additional file 1). The three genomes shared a core set of 3460 COGs and 6879 core genes. In addition, there were 8304 genes shared between *A. solani* HWC-168 and *A. arborescens* EGS 39–128, which was higher than that between *A. solani* HWC-168 and *A. brassicicola* ATCC 96836 (7301), and also higher than that between *A. arborescens* EGS 39–128 and *A. brassicicola* ATCC 96836 (7204). Taken together, these observations strongly indicate that significant gene variations including gene numbers and COGs exist in these closely related *Alternaria* strains, suggesting that these three *Alternaria* strains might have diverged in the genome evolution.

To annotate the predicted genes and assign Gene Ontology (GO) functions to them, predicted proteins from *A. arborescens* EGS39–128, *A. brassicicola* ATCC 96836 and *A. solani* HWC-168 were searched for homology to entries in the NCBI Ref Seq protein database, GO and InterPro databases using Blast2Go-PRO, respectively. As shown in Fig. 2, annotated genes contributing to the general function, amino acid transport and metabolism and carbohydrate transport and metabolism were predominant within the comparison of GO terms of three *Alternaria* genomes. However, further comparison of GO terms between these three *Alternaria* isolates revealed that the number of genes from each GO category was similar between *A. solani* HWC-168, *A. arborescens* EGS 39–128 and *A. brassicicola* ATCC 96836. In addition, we analyzed the GO functions of core genes and species-specific genes

Table 2 Summary of repetitive elements present in the genome of *A. solani* HWC-168

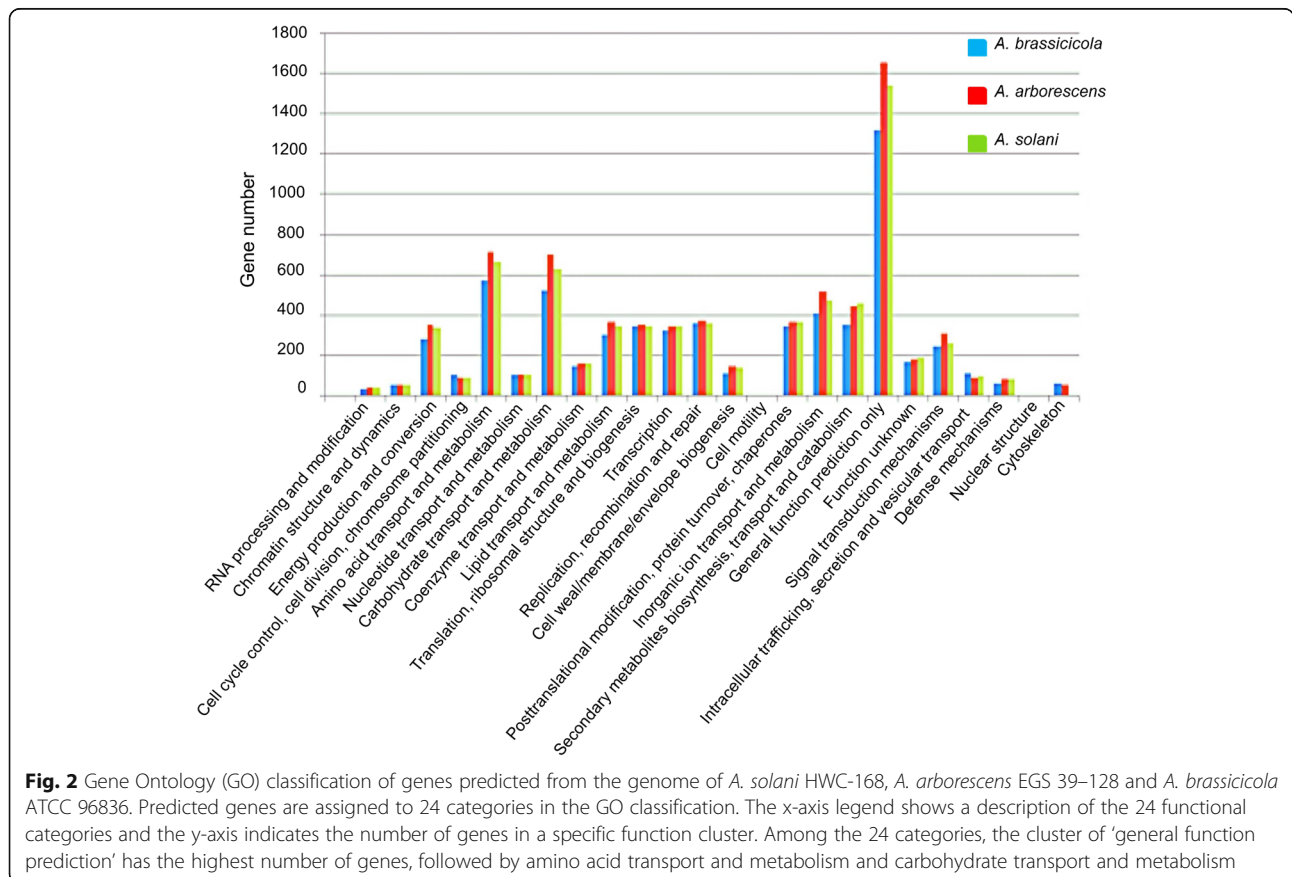
Repeat element	Superfamilies	Number of elements	Length occupied	% of assembled genome
DNA transposon		7633	798,198	2.43
	EnSpm/CACTA	1640	198,077	0.60
	Hobo-Activator (hAT)	1139	100,772	0.31
	Mariner/Tc1	901	148,218	0.45
	MuDR	754	60,332	0.18
	Harbinger	687	52,748	0.16
	Polinton	476	59,121	0.18
	Helitron	374	27,301	0.08
	Kolobok	233	33,732	0.10
	Sola	210	20,091	0.06
	Crypton	146	10,037	0.03
	piggyBac	132	8575	0.03
	Dada	116	9219	0.03
Endogenous Retrovirus		1069	69,620	0.21
	ERV1	414	27,788	0.08
	ERV2	360	23,610	0.07
	ERV3	102	6650	0.02
	ERV4	73	4385	0.01
LTR Retrotransposon		11,814	1,074,479	3.30
	Gypsy	6875	745,838	2.27
	Copia	3378	220,000	0.67
	BEL	989	58,924	0.18
	DIRS	339	21,781	0.07
Non-LTR Retrotransposon		4109	297,677	0.91
	L1	1049	66,695	0.20
	CR1	538	44,451	0.14
	R1	318	24,513	0.07
	Jockey	287	21,278	0.06
	RTE	232	15,218	0.05
	Tx1	211	14,176	0.04
	I	175	11,361	0.03
	Tad1	161	11,574	0.04
	L2	121	8125	0.02
	RTEX	106	8159	0.02
Pseudogene		94	16,566	0.05
	rRNA	57	13,659	0.04
	tRNA	37	2907	0.01
Satellite		145	14,774	0.04
	MSAT	40	6529	0.02
	SAT	63	4970	0.01
Integrated Virus		32	1760	0.005
	Caulimoviridae	29	1516	0.004
	DNA Virus	3	244	0.001
TOTAL		24,896	2,273,074	6.95



between *A. solani* HWC-168, *A. arborescens* EGS 39-128 and *A. brassicicola* ATCC 96836. A functional GO analysis determined that core genes and species-specific genes involved in general function dominated and that the second most abundant genes were related to translation, ribosomal structure and biogenesis (Fig. 3).

Secretome of *A. solani* HWC-168

By using SignalPv4.0, TMHMM-2.0, TargetPv1.01, and big-PI Predictor, we searched the genome of *A. solani* HWC-168 for secreted protein-encoding genes, which might act as effector candidate genes. Nine hundred seventy five secreted protein-encoding genes were



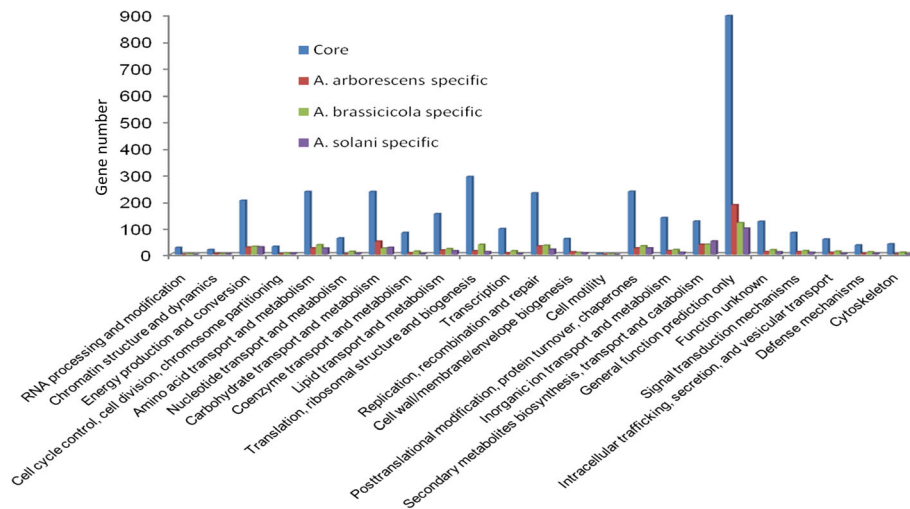


Fig. 3 Gene Ontology (GO) classification of core and species-specific genes identified from comparison of *A. solani* HWC-168, *A. arborescens* EGS 39–128 and *A. brassicicola* ATCC 96836 genomes. Predicted core and species-specific genes are assigned to 24 categories in the GO classification. The x-axis legend shows a description of the 24 functional categories and the y-axis indicates the number of genes in a specific function cluster. Among the 24 categories, the cluster of ‘general function prediction’ contains the highest number of core and species-specific genes, followed by translation, ribosomal structure and biogenesis

identified, which accounted for 9.4% of the total predicted genes.

Cell wall degrading enzymes

The majority of the secreted proteins were identified as cell wall degrading enzymes (CWDEs) involved in plant cell degradation. In addition, other enzymes that participate in various cellular metabolisms and non-enzyme proteins that maintain cellular energy and transport were also identified among these secreted proteins. Interestingly, we found that some secreted proteins identified from the secretome of *A. solani* HWC-168 were assigned to the same functional annotation but had differing functional classification (Additional file 2), suggesting that these secreted proteins may play important roles in various cellular activities.

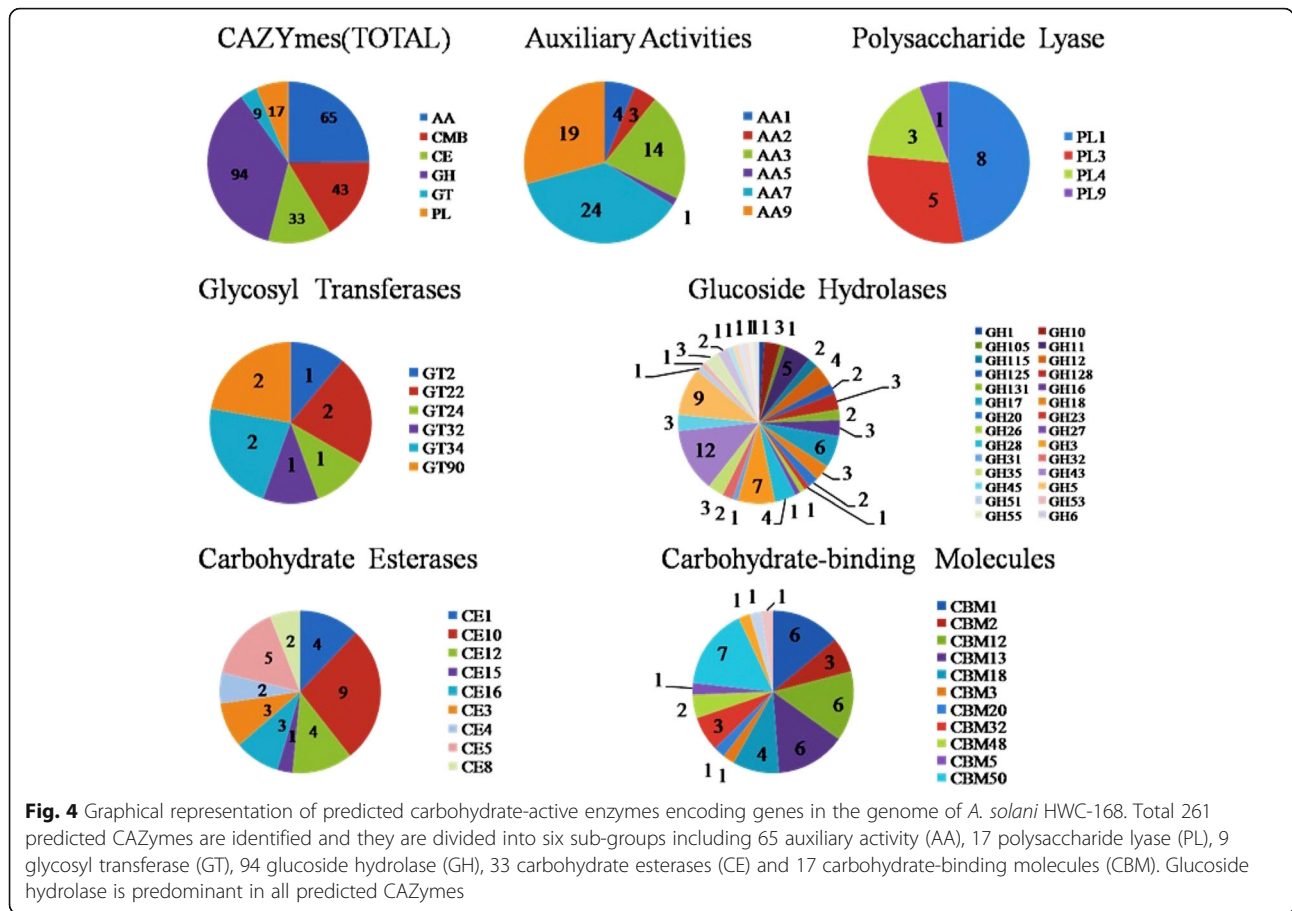
Carbohydrate-active enzymes and proteins with other predicted functions

The *A. solani* HWC-168 secretome possessed 261 secreted carbohydrate-active enzymes (CAZymes) with predicted activities (Fig. 4). One protease and one SnodProt elicitor belonging to the cerato-platanin protein (CPP) family were identified within the secretome of *A. solani* HWC-168. Surprisingly, a secreted protein exhibiting sequence homology to a superoxide dismutase was identified in the secretome of *A. solani* HWC-168. It has been reported that the superoxide dismutase is involved in inhibiting oxidative damage of pathogens and plant resistance [37, 38]. Furthermore, three trihydrophobins that are commonly found in the surface of aerial hyphae or fruiting body in fungi were predicted to be secreted [14, 15]. The

presence of trihydrophobins in the secretome of *A. solani* HWC-168 suggests their potential roles in fungal development, morphological differentiation and pathogenicity.

RxLx[EDQ] effector candidates

The RxLx[EDQ] motif functions as a host-targeting signal to deliver virulence proteins of *Plasmodium falciparum* into host cells [39]. The secretome of *A. solani* HWC-168 contained 119 secreted proteins possessing the RxLx[EDQ] motif (where x represents any amino acid). One of important criteria for effector prediction appears to be protein size less than 300 amino acids. Based on this criterion, 12 effector candidate proteins carrying RxLx[EDQ] motif within 120 amino acids downstream of N-terminal signal peptide were identified (Table 3). WEBLOGO analysis revealed that amino acids Arginine (R) in position 1 and Leucine (L) in position 3 and glutamic acid (E)/ aspartic acid (D)/glutamine(Q) in the 5 position were highly conserved in the RxLx [EDQ] motif. By contrast, bilateral amino acid sequences surrounding the RxLx[EDQ] motif were not conserved and tended to be highly variable (Fig. 5a). In addition, we found that the continuous aspartic acid (D), glutamic acid (E) and glutamine (Q) residues were present in the downstream of the RxLx[EDQ] motif but with variable locations (Fig. 5b). Due to the important roles of RxLR effectors in the pathogenicity of *Phytophthora infestans*, functional analysis of the RxLx[EDQ] motif-containing proteins in the secretome of *A. solani* HWC-168 will be the focus for future research.



Unique secreted proteins

We observed that 27 predicted genes encoding secreted proteins were completely absent in the genome of *A. arborescens* and *A. brassicicola* (Additional file 3). As a consequence, the function of these secreted proteins remains unknown due to the lack of homology with known proteins. Interestingly, from 27 species-specific

genes we identified 3 pairs of neighbor genes that reside on three different scaffolds: scaffold 18, scaffold 21 and scaffold 8, respectively (Additional file 4). These findings suggest that the presence of these species-specific secreted protein-encoding genes in the genome of *A. solani* HWC-168 may have originated by two possibilities: either the genome of *A. solani* HWC-168 possesses

Table 3 List of predicted effector candidates carrying the RxLx[EDQ] motif

Name	Size	Start of sequence
ASLO_253	148	MKFTLAIVALASVATTALANREWTYNDSHRAVAVTALKQITAKHAHLCKR
ASLO_323	134	MKLAIAALFASITAAAPTATPDVHGDPFETVTISNFVYVGVNGYPQIDFH
ASLO_2101	114	MQIMNLAVLAATLATVGAWTLDDYGKWANNWRDNLNGVHKVHESCAER
ASLO_4082	266	MKFLAIIAAQLATALPVAKEACSSDITCSATKANPQIFDVASQQLDNS
ASLO_5583	205	MVSFRNLFTAAMALSVPVAAVLTPAQIVDNIRILTQKSQALQAPAQSITI
ASLO_5663	199	MASSIPDHWLWGLGVFTFIQVQVSHGLHTIRALTEIRNPQNMPQORRA
ASLO_6610	169	MLGRTVFAATFFALAQFAMASPPSCLLGAVNQYEDPSDIKAVCKARNLSE
ASLO_6668	183	MFLPTALLALVHLALPALSHASPQALVSSDWEMSLVPRHQFLRQLSDL
ASLO_8389	252	MYSKTAIVTFFAGFAAAQIHAPVGEPSGNPITRPLNEWPTCEQFTITWQ
ASLO_8909	270	MAKLIDLSTEVFLIVAYFTSGDASDVQALLHLCRTSRMLVAVAQPALYT
ASLO_9385	163	MHFSVIFSAVFAATAMAAPASLDSRGEDECVPDSYITSDYTLTSPSTSGS
ASLO_10144	244	MLSNLMNRFALPLAILAFFLSFANGLPHDALIARRTTNLRILPLGDSITW

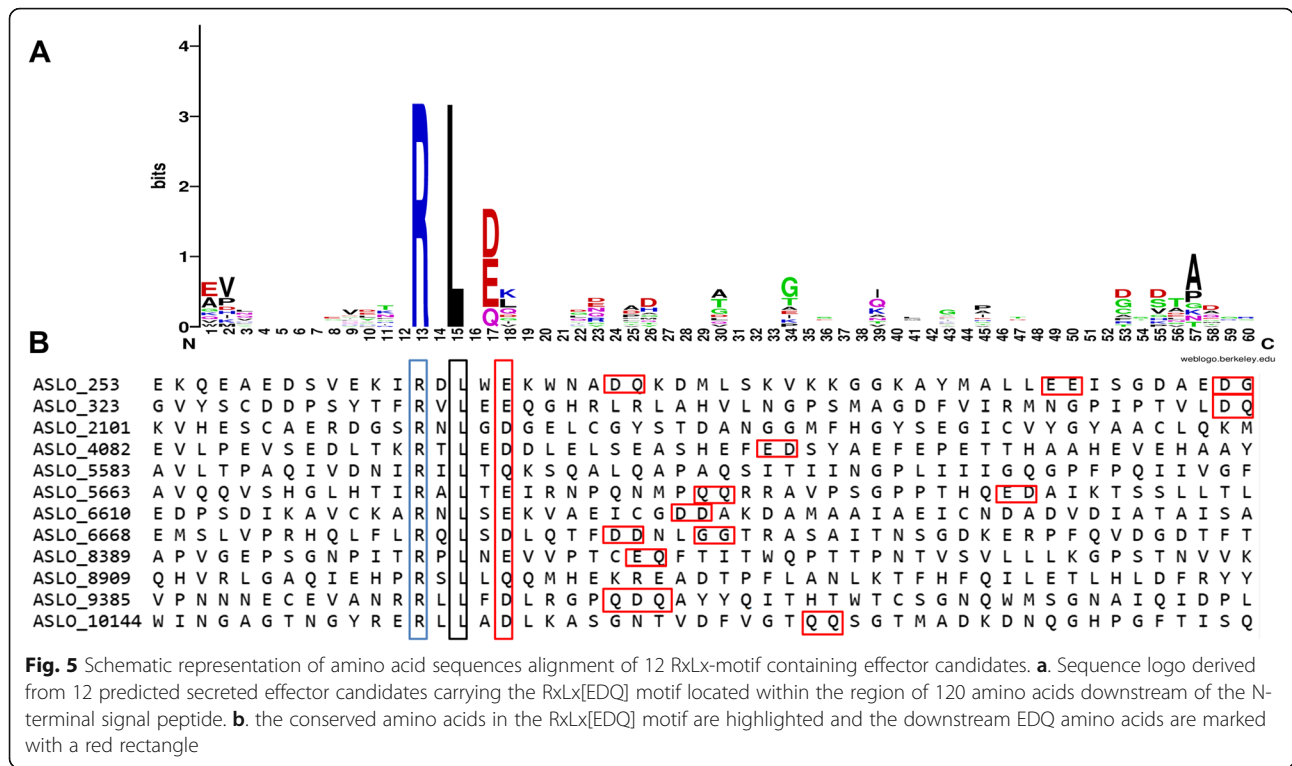


Fig. 5 Schematic representation of amino acid sequences alignment of 12 RxLx-motif containing effector candidates. **a.** Sequence logo derived from 12 predicted secreted effector candidates carrying the RxLx[EDQ] motif located within the region of 120 amino acids downstream of the N-terminal signal peptide. **b.** the conserved amino acids in the RxLx[EDQ] motif are highlighted and the downstream EDQ amino acids are marked with a red rectangle

a large genomic fragment that is missing in other *Alternaria* genomes or the genomic databases of *A. arborescens* and *A. brassicicola* are incomplete because only their draft genomes are reported, which has resulted in the absence of these secreted proteins. Functional analysis of these species-specific secreted proteins in *A. solani* HWC-168 is under way in our laboratory.

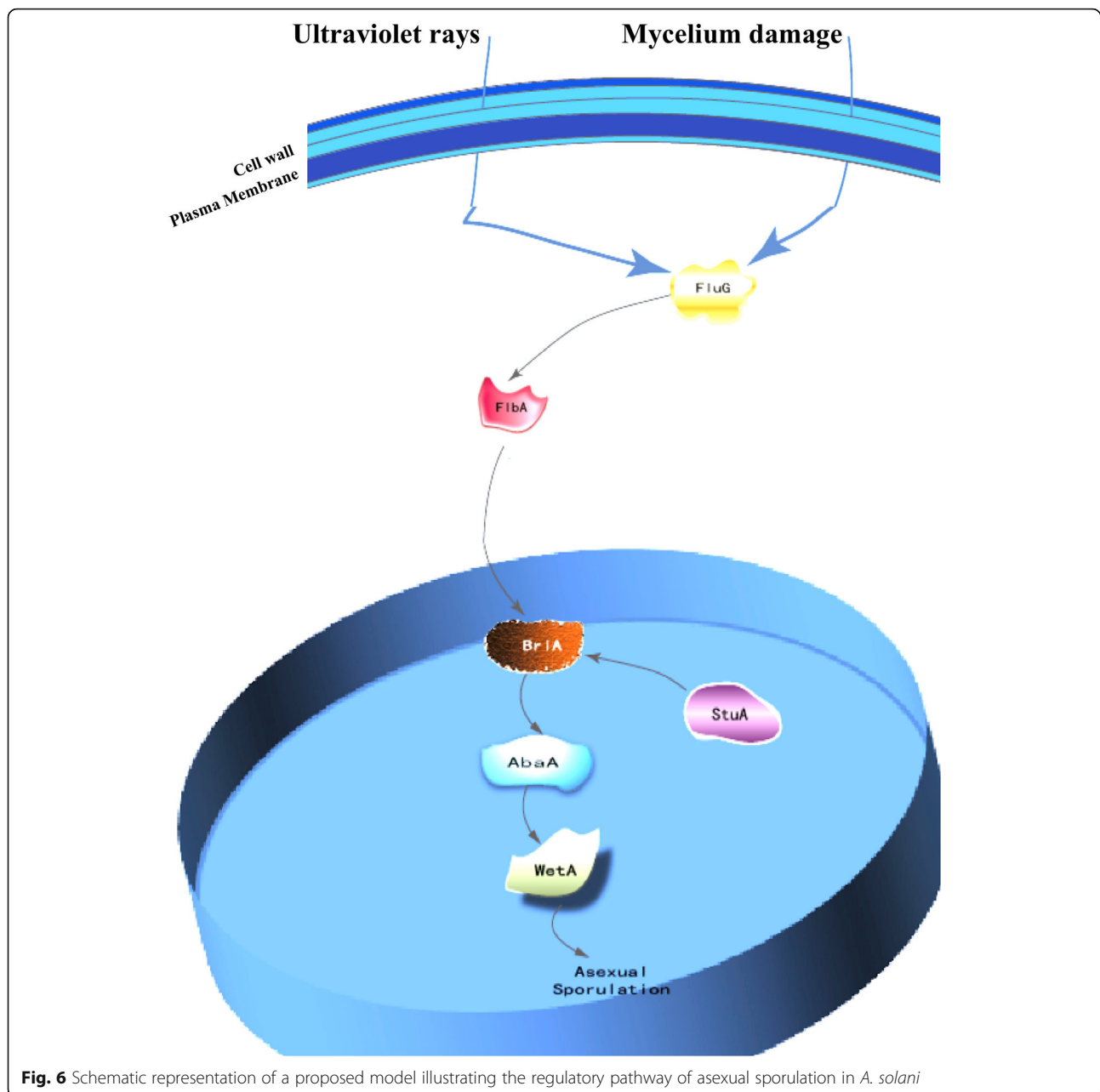
Prediction of conidiation-related genes

Our earlier studies revealed that it was difficult to induce conidiation in our *A. solani* isolates under artificial culturing condition. However, *A. solani* HWC-168 is capable of yielding copious conidiospores when its mycelia are radiated by ultraviolet (UV light) (Additional file 5). To identify genes involved in conidiation, we retrieved the central regulatory genes participating in the conidiation from the genome of *Aspergillus nidulans* and blasted the *brlA* sequence and other sporulation related genes, such as *abaA*, *wetA*, *stuA*, *fluG*, *flbA*, *flbC*, *flbD*, *flbE*, *medA* and *fadA*, to the predicted protein database of *A. solani*. Our results showed that homologous genes including *fluG*, *flbA*, *flbC*, *flbE*, *brlA*, *stuA*, *abaA*, *wetA*, *medA* and *fadA* existed in the genome of *A. solani*-HWC168. Based on the proposed conidiation model in *Aspergillus nidulans* and the identified conidiation-related genes in *A. solani* HWC-168, we propose a potential conidiation pathway in *A. solani* HWC-168 (Fig. 6).

Discussion

Pathogenic *A. solani* strains are increasingly posing a critical threat to world food security. Sequencing the whole genome of *A. solani* is a key step to facilitate the study of the molecular mechanisms underlying the interaction between potato and *A. solani*. Here, we presented the completed genome sequence and annotation of *A. solani* HWC-168 generated by advanced next-generation Illumina sequencing technology. The quality of the genome sequence was guaranteed by using two individual sequencing libraries. The genome sequence data of *A. solani* HWC-168 has the potential to facilitate a future study on the molecular basis of *A. solani* virulence.

Genomes of three *A. solani* isolates have been sequenced in the past [30–32]. The assembled genome size of *A. solani* ranges from 32.6 to 32.9 Mb. Our sequenced *A. solani* HWC-168 produced a genome size of 32.8 Mb, which compares favorably with the reported genome size of *A. solani* altNL03003 (Table 1). The genome of *A. solani* altNL03003 had been sequenced using the long-read Pacific Biosciences (PacBio) sequencing technology, which provided a gapless genome assembly. Although we sequenced the genome of *A. solani* HWC-168 using the second-generation sequencing technology, the same genome size was produced with *A. solani* altNL03003 but the assembled contig number of *A. solani* HWC-168 being higher than that of *A. solani* altNL03003. This suggests a high-quality genome assembly of altNL03003 has



been obtained. However, we were not able to compare our predicted genes with those of *A. solani* altNL03003 because of the lack of annotation data of *A. solani* altNL03003. By searching our predicted RxLx[EDQ] effector candidates and conidiation-related genes in the genome of *A. solani* altNL03003, we found that all of them were present in the genome of *A. solani* altNL03003 (Additional file 3 and unpublished data). This observation strongly suggests that the genome annotation of *A. solani* HWC-168 is accurate. It has been reported that the repeat content in the genome of *A.*

solani CBS109157 is relatively low with only 1.5% [31]. Surprisingly, we found that the percentage of repeat content of *A. solani* HWC-168 was relatively high with 6.95% although both of them have similar genome size. This apparent discrepancy requires future study to identify repeat contents from the gapless assembled genome of *A. solani* altNL03003.

Asexual sporulation is a common reproduction strategy in filamentous fungi. Although they vary in morphology and function, conidia in higher fungi are developed from specialized sporogenous cells or asexual propagules. The

conidiation-related processes are complicated, including the space-time regulation of conidiation-related genes, cell specialization and cell signal transduction, etc. The genetic mechanism of conidiation in *Aspergillus nidulans* has been well studied [40, 41]. However, the molecular basis underlying conidiation in *A. solani* remains unclear. Elucidation of genes regulating the conidiation process is essential to our understanding of asexual reproduction in *A. solani* species. Here, we first presented the evidence that the central regulatory factors of conidiation identified from *Aspergillus nidulans* including *abaA*, *wetA*, *StuA*, *FluG* and *FlbA* genes are present in the genome of *A. solani* HWC-168. This suggests a similar molecular mechanism of sporulation is employed by *A. solani*; however, these homologous conidiation-related genes in *A. solani* are putative and functional confirmation is required. We are examining the expression profiles of predicted conidiation-related genes (unpublished data). We are confident that future studies designed to elucidate the molecular basis of conidiation will provide the impetus to develop novel strategies to prevent sporulation in order to control disease development caused by *A. solani* on potato.

The secreted fungal enzymes in pathogenic fungi play important roles in pathogenicity. Here, we found that the secreted enzymes in *A. solani* HWC-168 contain a large number of cellulases and pectinases. Previous studies showed that cellulases and pectinases in *Alternaria* species play key roles in degrading the plant cell wall during infection [42–44]. Thus, we proposed that cellulases and pectinases in *A. solani* play important roles in infecting the host and causing degradation of host cell wall. In our work, a total of 975 predicted secreted proteins were identified in the genome of *A. solani* HWC-168, comprising 261 CAZymes, 119 RxLx[EDQ] motif containing secreted proteins and 27 species-specific secreted proteins. It remains unknown how these species-specific secreted proteins contribute to the pathogenicity of *A. solani* HWC-168. However, we speculate that some of the proteins might function inside plant cells, which has been widely reported in the effector proteins of rust and oomycete plant pathogens [45–48]. Translocation of rust and oomycete effector proteins into plant cell largely depends on the conserved RxLx-motif [46, 47]. In the secretome of *A. solani* HWC-168, 12 RxLx-motif containing effector candidate proteins were found, which indicates that they might serve as virulence factors during *A. solani* infection. Recent reports showed that RxLR effectors from various fungal pathogens are involved in virulence, which will broaden the implications of our findings [49]. The RxLx-motif containing effectors involving in the pathogenicity during the interaction between *A. solani* HWC-168 and potato will be further investigated.

Conclusions

In this study we developed and annotated the complete genome sequence of *A. solani* HWC-168, and predicted the conidiation-related genes and the secretome that contains the virulence-related genes. To our best knowledge, this is the first time that the effector candidate genes and conidiation-related genes have been predicted in the genome of *A. solani*, which will facilitate the identification and functional analysis of conidiation- and virulence-related genes in *A. solani*. Availability of the genome sequence of *A. solani* HWC-168 and its host potato coupled with advanced genetic and molecular approaches will enable an understanding of the molecular mechanisms underlying the *A. solani*-potato pathosystem.

Methods

Strain and culture conditions

The strain *A. solani* HWC-168 was isolated from the infected leaves of potato in Weichang County Hebei province in China. All *Alternaria* isolates were cultured on potato dextrose agar (PDA). Mycelia were obtained by growing the isolate for at least 7 days on PDA plates.

Genomic DNA preparation and library construction

The mycelia were harvested by filtration and frozen at -20°C . DNA was extracted from the mycelia according to a modified etyltrimethylammonium bromide procedure (CTAB) [50]. Following DNA fragmentation, we constructed two genomic sequencing libraries: one is a paired-end library with 500 bp inserts and another is a mate-pair library with 5 kp insertion fragments. The paired-end library was constructed using the Paired-End DNA sample Prep Kit (Illumina, USA) following the protocols provided by the manufacturer. The mate-pair library was constructed using the Nexera Mate Pair Library Prep Kit (Illumina, USA) following the protocols provided by the manufacturer.

Genome sequencing and assembly

Two constructed libraries were sequenced by using the Illumina GA II technology (Illumina, USA) HiSeq 2000 platforms at the Beijing Genomics Institute using the WGS (whole genome sequencing) method. The read length is 150 bp. Low-quality data containing a quality value of less than 20 and short reads (length 35 bp) were filtered from raw data by Dynamic Trim and Length Sort Perl program in the SolexaQA software [51]. SOAPdenovo software (<http://soap.genomics.org.cn>) was used to assemble sequences and gaps were merged by SOAP Gap Closer software (<http://soap.genomics.org.cn>) [52]. ORFs (open reading frames) were predicted by Augustus 2.5.5 software [53], and were aligned with homologous proteins

in the NCBI database (<http://www.ncbi.nlm.nih.gov/>). All confirmed ORFs were aligned with COG (Clusters of Orthologous Groups) in the NCBI database, and were classified by function based on alignment results and classification standards of COG. Repetitive elements were identified by CENSOR (<http://www.girinst.org/censor>) following the default parameters.

Genome comparison

The genome comparison was performed among *A. solani* HWC-168, *A. arborescens* and *A. brassicicola*. Multiple sequence alignments of genomes were performed with Mugsy [54]. The homologous genes were aligned using PanOCT software [55] by designating the parameter values: protein sequence with > 60% identity, aligned length > 30% and E value less than $1e-5$, the Intergenic distance was calculated using the method described previously [56].

Secreted protein annotation and prediction

The secreted proteins putatively encoded in the genome of *A. solani* HWC-168 were predicted by SignalPv4.0 (<http://www.cbs.dtu.dk/services/SignalP/>), TMHMM-2.0 (<http://www.cbs.dtu.dk/services/TMHMM-2.0/>), TargetPV1.01 (<http://www.cbs.dtu.dk/services/TargetP/>), and Big-pi (http://mendel.imp.ac.at/gpi/fungi_server.html). In detail, we followed the effector prediction pipeline described previously [57]. We first searched the ones with the presence of an N-terminal signal peptide through signalIP4.1. Then, we excluded the ones with a predicted transmembrane domains using TMHMM-2.0. Next, we detected the presence of subcellular localization signals using TargetP and glycosylphosphatidylinositol (GPI) anchor to the membrane and filtered out the ones with mitochondrial localization and then the ones with GPI. The secreted proteins in *A. arborescens* and *A. brassicicola* were predicted by using the same method. The secreted proteins in *A. solani* HWC-168 were used as inquiring sequences to search against the secretomes of *A. arborescens* and *A. brassicicola* by BLASTP. The parameter values were designated as E-value < 10^{-5} and identity > 30%. The secreted proteins with no homologous ones in *A. arborescens* and *A. brassicicola* were defined as species-specific proteins in *A. solani* HWC-168.

Carbohydrate-active enzyme annotation

All putative proteins of *A. solani* HWC-168 were searched against entries in the CAZy database by using CAZymes Analysis Toolkit [58] using the Carbohydrate Active Enzymes (CAZy) database (<http://www.cazy.org>). The parameter values were in default on the website. All identified proteins were then manually retrieved.

Prediction of proteins with a RxLx[EDQ]

The predicted secreted proteins in *A. solani* HWC-168 were examined with the presence of the conserved host-targeting motif RxLx[EDQ] by using the MEME prediction server (<http://meme-suite.org/tools/meme>) with default parameters. The amino acids in the conserved RxLx[EDQ] motif were aligned by WEBLOGO software [59].

Additional files

Additional file 1: Venn-diagram showing the cluster of orthologous group (COGs) genes for related three strains including *A. solani*, *A. arborescens* and *A. brassicicola*. Ortholog clusters were computed by using PanOCT with set parameter cutoffs (E value < 10^{-5} ; match length > 30%; identity > 60%). (DOCX 137 kb)

Additional file 2: Representative enzymes with the same function but involving in different biological activities. (DOCX 14 kb)

Additional file 3: Twenty seven species-specific secreted proteins based on the prediction. (DOCX 17 kb)

Additional file 4: Three pairs of specific neighbor genes reside on three different scaffolds. (DOCX 14 kb)

Additional file 5: Conidia and conidiophores formed by *A. solani* HWC-168 were visualized under microscopy. (DOCX 154 kb)

Abbreviations

CAZy: Carbohydrate-active enzymes; COG: Clusters of orthologous groups; CPP: Cerato-platanin protein; CTAB: Etyltrimethylammonium bromide; CWDEs: Cell wall degrading enzymes; GPI: Glycosylphosphatidylinositol

Acknowledgments

We thank Dr. Gordon Gropp (Saskatoon Development and Research Centre of Agriculture and Agri-Food Canada) and Dr. Likui Zhang (Yangzhou University) for the critical reading of our manuscript.

Funding

This research was supported by the Earmarked Fund for Modern Agro-industry Technology Research System (CARS-09-P18), the National Key Research and Development Program of China (2018YFD0200806) and The Earmarked Fund for Modern Agro-industry Technology Research System in Hebei Province, China (HBC2018080205). The funding body has no role in the design of the study and collection, analysis and interpretation and in writing the manuscript.

Availability of data and materials

The datasets including genome sequence and assembly are available in NCBI GenBank under accession number JRVW000000000.1. The datasets including predicted genes and conidiation-related genes are available from the corresponding author upon reasonable request. The rest of datasets generated or analyzed in this work are included in this published article. Strains were collected and taken according to the guidelines of the Chinese "Biosafety Management Regulations for Pathogenic Microbiological Laboratory".

Authors' contributions

DZ, JHZ, ZHY and LM conceived and designed the experiments. DZ, JYH and PH performed the experiments and PH, JHZ, LM and ZHY analyzed the data. DZ, LM, JHZ and ZHY drafted the manuscript. All authors read and approved the final manuscript.

Ethics approval and consent to participate

Not applicable

Consent for publication

Not applicable

Competing interests

The authors declare that they have no competing interests.

Publisher's Note

Springer Nature remains neutral with regard to jurisdictional claims in published maps and institutional affiliations.

Author details

¹Center of Plant Disease and Plant Pests of Hebei Province, College of Plant Protection, Hebei Agricultural University, Baoding 071001, China. ²Saskatoon Research and Development Centre, Agriculture and Agri-Food Canada, Saskatoon, SK S7N0X2, Canada.

Received: 8 May 2018 Accepted: 22 October 2018

Published online: 06 November 2018

References

- Haware MP. Assessment of losses due to early blight (*Alternaria solani*) of potato. *Mycopathol Mycol Appl.* 1971;43(3):341–2.
- Brian PW, Curtis PJ, Hemming HG, Wright JM. Alternaric acid, a biologically active metabolic product of the fungus *Alternaria solani*. *Nature.* 1949;164(4169):534.
- Brian PW, Curtis PJ, Hemming HG, Jefferys EG, Wright JM. Alternaric acid; a biologically active metabolic product of *Alternaria solani* (Ell. & Mart.) Jones & Grout; its production, isolation and antifungal properties. *J Gen Microbiol.* 1951;5(4):619–32.
- GamboaAngulo MM, AlejosGonzalez F, PenaRodriguez LM. Homozinnol, a new phytotoxic metabolite from *Alternaria solani*. *J Agric Food Chem.* 1997; 45(1):282–5.
- Moreno-Escobar J, Puc-Carrillo A, Caceres-Farfan M, Pena-Rodriguez LM, Gamboa-Angulo MM. Two new zinnol-related phytotoxins from *Alternaria solani*. *Nat Prod Res.* 2005;19(6):603–7.
- Ai HL, Zhang LM, Chen YP, Zi SH, Xiang H, Zhao DK, Shen Y. Two new compounds from an endophytic fungus *Alternaria solani*. *J Asian Nat Prod Res.* 2012;14(12):1144–8.
- Andersen B, Dongo A, Pryor BM. Secondary metabolite profiling of *Alternaria dauci*, *A. porri*, *A. solani*, and *A. tomatophila*. *Mycol Res.* 2008;112:241–50.
- Prasad B, Dutt BL. Inducing sporulation in *Alternaria solani*. II. Effect of light. *Mycopathol Mycol Appl.* 1974;54(1):47–54.
- Prasad B, Dutt BL, Nagaich BB. Inducing sporulation in *Alternaria solani*. I. Effect of water treatment. *Mycopathol Mycol Appl.* 1973;49(2):141–6.
- Rich S, Tomlinson H. Effects of ozone on conidiophores and conidia of *alternaria solani*. *Phytopathology.* 1968;58(4):444–6.
- Singh BM. Inducing sporulation in different strains of *Alternaria solani*. II. Effect of ultraviolet light. *Mycopathol Mycol Appl.* 1967;32(2):163–71.
- Leiminger JH, Auinger HJ, Wenig M, Bahnweg G, Hausladen H. Genetic variability among *Alternaria solani* isolates from potatoes in southern Germany based on RAPD-profiles. *J Plant Dis Protect.* 2013;120(4):164–72.
- Lourenco V, Rodrigues TTM, Campos AMD, Braganca CAD, Scheuermann KK, Reis A, Brommonschenkel SH, Maffia LA, Mizubuti ESG. Genetic structure of the population of *Alternaria solani* in Brazil. *J Phytopathol.* 2011;159(4):233–40.
- Tymon L, Cummings TF, Johnson DA. Pathogenicity and aggressiveness of *Alternaria solani*, *A. alternata*, and *A. triticina* on potato. *Phytopathology.* 2013;103(6):149–50.
- van der Waals JE, Korsten L, Slippers B. Genetic diversity among *Alternaria solani* isolates from potatoes in South Africa. *Plant Dis.* 2004;88(9):959–64.
- Varma PK, Singh H, Gandhi SK, Chaudhary K. Variability among *Alternaria solani* isolates associated with early blight of tomato. *Commun Agric Appl Biol Sci.* 2006;71(4):37–46.
- Weber B, Halterman DA. Analysis of genetic and pathogenic variation of *Alternaria solani* from a potato production region. *Eur J Plant Pathol.* 2012; 134(4):847–58.
- Park HS, Yu JH. Genetic control of asexual sporulation in filamentous fungi. *Curr Opin Microbiol.* 2012;15(6):669–77.
- Bahn YS, Xue H, Idnum A, Rutherford JC, Heitman J, Cardenas ME. Sensing the environment: lessons from fungi. *Nat Rev Microbiol.* 2007;5:57–69.
- Etebeste O, Garzia A, Espeso EA, Uqalde U. *Aspergillus nidulans* asexual development: making the most of cellular modules. *Trends Microbiol.* 2010; 17(12):569–72.
- Son H, Kim MG, Min K, Seo YS, Lim JY, Choi GJ, Kim JC, Chae SK, Lee YW. AbaA regulates conidiogenesis in the ascomycete fungus *Fusarium graminearum*. *PLoS One.* 2013;8(9):e72915.
- Adams T, Boylan MT, Timberlake WE. BrlA is necessary and sufficient to direct conidiophore development in *Aspergillus nidulans*. *Cell.* 1988;54(3): 353–62.
- Ruger-Herreros C, Rodríguez-Romero J, Fernández-Barranco R, Olmedo M, Fischer R, Corrochano LM, Canovas D. Regulation of conidiation by light in *Aspergillus nidulans*. *Genetics.* 2011;188(4):809–22.
- Mirabito PM, Adams TH, Timberlake WE. Interactions of three sequentially expressed genes control temporal and spatial specificity in *aspergillus* development. *Cell.* 1989;57(5):859–68.
- Sewall TC, Mims CW, Timberlake WE. Conidium differentiation in *Aspergillus nidulans* wild-type and wet-white (wetA) mutant strains. *Dev Biol.* 1990; 138(2):499–508.
- Marshall MA, Timberlake WE. *Aspergillus nidulans* wetA activates spore-specific gene expression. *Mol Cell Biol.* 1991;11(1):55–62.
- Wieser J, Lee BN, Fondon JW, Adams TH. Genetic requirements for initiating asexual development in *Aspergillus nidulans*. *Curr Genet.* 1994;27(1):62–9.
- Wu J, Miller BL. *Aspergillus* asexual reproduction and sexual reproduction are differentially affected by transcriptional and translational mechanisms regulating stunted gene expression. *Mol Cell Biol.* 1997;17(10):6191–201.
- Miller KY, Wu J, Miller BL. StuA is required for cell pattern formation in *aspergillus*. *Genes Dev.* 1992;6(9):1770–82.
- Dang HX, Pryor B, Peever T, Lawrenc CB. The *Alternaria* genomes database: a comprehensive resource for a fungal genus comprised of saprophytes, plant pathogens, and allergenic species. *BMC Genomics.* 2015;16:239–50.
- Woudenberg JHC, Seidl MF, Groenewald JZ, de Vries M, Stielow JB, Thomma BPHJ, Crous PW. *Alternaria* section *Alternaria*: species, *formae speciales* or pathotypes? *Stud Mycol.* 2015;82:1–21.
- Wolters PJ, Faino L, van den Bosch TBM, Evenhuis B, Visser RGF, Seidl MF, Vleeshouwers VGAA. Gapless genome assembly of the potato and tomato early blight pathogen *Alternaria solani*. *Mol Plant-Microbe Interact.* 2018; 31(7):692–4.
- Huang K, Zhong Y, Li Y, Zheng D, Cheng ZM. Genome-wide identification and expression analysis of the apple ASR gene family in response to *Alternaria alternata* f. sp. mali. *Genome.* 2016;59(10):866–78.
- Bihon W, Cloete M, Gerrano AS, Oelofse D, Adebola P. Draft genome sequence of *Alternaria alternata* isolated from onion leaves in South Africa. *Genome Announc.* 2016;4(5):1022–16.
- Nguyen HD, Lewis CT, Levesque CA, Grafenhan T. Draft genome sequence of *Alternaria alternata* ATCC 34957. *Genome Announc.* 2016;4(1):1554–15.
- Wang M, Sun X, Yu D, Xu J, Chung K, Li H. Genomic and transcriptomic analyses of the tangerine pathotype of *Alternaria alternata* in response to oxidative stress. *Sci Rep.* 2016;6(1):1–11.
- Lightfoot DJ, Mcgrann GR, Able AJ. The role of cytosolic superoxide dismutase in barley-pathogen interactions. *Mol Plant Pathol.* 2017;18(3):323–35.
- Lu F, Liang X, Lu H, Li Q, chen Q, Zhang P, Li K, Liu G, Yan W, Song J, Duan C, Zhang L. Overproduction of superoxide dismutase and catalase confers cassava resistance to *Tetrazychnus cinnabarinus*. *Sci Rep.* 2017;7:40179.
- Marti M, Good RT, Rug M, Knuepfer E, Cowman AF. Targeting malaria virulence and remodeling proteins to the host erythrocyte. *Science.* 2004;10: 1930–3.
- Emri T, Molnar Z, Pusztahelyi T, Varcza Z, Pocsí I. The fluG-BrlA pathway contributes to the initialisation of autolysis in submerged *Aspergillus nidulans* cultures. *Mycol Re.* 2005;109:757–63.
- Rodrigues TTMS, Maffia LA, Dhingra OD, Mizubuti ESG. In vitro production of conidia of *Alternaria solani*. *Trop Plant Pathol.* 2010;35(4):203–12.
- Goatley JL. Production of exocellular polysaccharides by *Alternaria solani*. *Can J Microbiol.* 1968;14(10):1063–8.
- Shahbazi H, Aminian H, Sahebani N, Halterman DA. Activity of beta-1,3-glucanase and beta-1,4-glucanase in two potato cultivars following challenge by the fungal pathogen *Alternaria solani*. *Phytoparasitica.* 2011; 39(5):455–60.
- Cho Y, Jang M, Srivastava A, Jang JH, Soung NK, Ko SK, Kang DO, Ahn JS, Kim BY. A pectate lyase-coding gene abundantly expressed during early stages of infection is required for full virulence in *Alternaria brassicicola*. *PLoS One.* 2015;10(5):e0127140.
- Kemen E, Kemen AC, Rafigi M, Hempel U, Mendgen K, Hahn K, Hahn M, Voegelé RT. Identification of a protein from rust fungi transferred from haustoria into infected plant cells. *Mol Plant-Microbe Interact.* 2005;18(11): 1130–9.
- Dodds PN, Lawrence G, Catanzariti AM, Ayliffe MA, Ellis JG. The *Melampsora lini* AvrL567 avirulence genes are expressed in haustoria and their products are recognized inside plant cells. *Plant Cell.* 2004;16(3):755–68.
- Birch PRJ, Rehmany AP, Pritchard L, Kamoun S, Beynon JL. Trafficking arms: oomycete effectors enter host plant cells. *Trends Microbiol.* 2006;14(1):8–11.

48. Mendgen K, Hahn M. Plant infection and the establishment of fungal biotrophy. *Trends Plant Sci.* 2002;7(8):352–6.
49. Choi J, Park J, Kim D, Jung K, Kang S, Lee YH. Fungal Secretome database: integrated platform for annotation of fungal secretomes. *BMC Genomics.* 2010;11:105.
50. Storchova H, Hrdlickova R, Chrtek J, Tetera M, Fitze D, Fehrer J. An improved method of DNA isolation from plants collected in the field and conserved in saturated NaCl/CTAB solution. *Taxon.* 2000;49(1):79–84.
51. Cox MP, Peterson DA, Biggs PJ. SolexaQA: at-a-glance quality assessment of Illumina second-generation sequencing data. *BMC Bioinformatics.* 2010;11:485.
52. Luo R, Liu B, Xie Y, Li Z, Huang W, Yuan J, He G, Chen Y, Pan Q, Liu Y, Tang J, Wu G, Zhang H, Shi Y, Liu Y, Yu C, Wang B, Lu Y, Han C, Cheung DW, Yiu SM, Peng S, Xiaoqian Z, Liu G, Liao X, Li Y, Yang H, Wang J, Lam TW, Wang J. SOAPdenovo2: an empirically improved memory-efficient short-read de novo assembler. *Gigascience.* 2012;1(1):18.
53. Stanke M, Tzvetkova A, Morgenstern B. AUGUSTUS at EGASP: using EST, protein and genomic alignments for improved gene prediction in the human genome. *Genome Biol.* 2006;7:11.
54. Angiuoli SV, Salzberg SL. Mugsy: fast multiple alignment of closely related whole genomes. *Bioinformatics.* 2011;27(3):334–42.
55. Fouts DE, Brinkac L, Beck E, Inman J, Sutton G. PanOCT: automated clustering of orthologs using conserved gene neighborhood for pan-genomic analysis of bacterial strains and closely related species. *Nucleic Acids Res.* 2012;40(22):e172.
56. Nelson CE, Hersh BM, Carroll SB. The regulatory content of intergenic DNA shapes genome architecture. *Genome Biol.* 2004;5(4):R25.
57. Haddadi P, Ma L, Wang H, Borhan MH. Genome-wide transcriptomic analyses provide insights into the lifestyle transition and effector repertoire of *Leptosphaeria maculans* during the colonization of *Brassica napus* seedlings. *Mol Plant Pathol.* 2016;17(8):1196–210.
58. Park BH, Karpinets TV, Syed MH, Leuze MR, Uberbacher EC. CAZymes analysis toolkit (CAT): web service for searching and analyzing carbohydrate-active enzymes in a newly sequenced organism using CAZy database. *Glycobiology.* 2010;20(12):1574–84.
59. Crook GE, Hon G, Chandonia JM, Brenner SE. WebLogo: A sequence Logo generator. *Genome Res.* 2004;14(6):1188–90.

Ready to submit your research? Choose BMC and benefit from:

- fast, convenient online submission
- thorough peer review by experienced researchers in your field
- rapid publication on acceptance
- support for research data, including large and complex data types
- gold Open Access which fosters wider collaboration and increased citations
- maximum visibility for your research: over 100M website views per year

At BMC, research is always in progress.

Learn more biomedcentral.com/submissions

